# Echoes of impact: A petrographic analysis and classification of impact breccias from Hummeln, Sweden

*Ludvig Svensson*

**Dissertations in Geology at Lund University,**
**Bachelor's thesis, no 687**
**(15 hp/ECTS credits)**

**Department of Geology**
**Lund University**
**2024**

# Echoes of impact: A petrographic analysis and classification of impact breccias from Hummeln, Sweden

Bachelor's thesis

Ludvig Svensson

Department of Geology
Lund University
2024

# Contents



**Cover Picture:** Picture taken at lake Hummeln, nice view! From Ludvig Svensson

# Abstract

LUDVIG SVENSSON

Svensson, L., 2024: Echoes of impact: A petrographic analysis and classification of impact breccias from Hummeln, Sweden. *Dissertations in Geology at Lund University*, No. 687, 25 pp. 15 hp (15 ECTS credits) .

**Abstract:** The Hummeln structure is a relatively recently confirmed impact structure located in the northeastern part of the province of Småland in Sweden (57.37347°N 16.25084°Ö). Due to its relatively recent confirmation, detailed petrographic studies regarding shock metamorphism and shock metamorphic features in the Hummeln-1 drill core are lacking. The drill core is the only drill core from the structure and reached about ~164.25 meters, measured from the lake surface. This study describes, classifies, and discusses three rock types from the lower part of the drill core, and their relationship to the impact event. Three thin sections from these rock types were analysed using polarizing microscopy, two of which were also analysed using scanning electron microscopy (SEM). From the top down, the first rock (Breccia 1) is a monomict cataclastic impact breccia located between 159.14 and 160.55 meters. The second rock (Breccia 2) is a polymict suevitic impact breccia (160.45-160.75 m) that contain shock metamorphic features in quartz in the form of planar fractures (PFs) and planar deformation features (PDFs). The third breccia (Breccia 3) is a polymict lithic impact breccia located between 160.75 and 161.4 meters. These breccias might have formed through slumping during the modification stage of impact crater formation, which means that they would constitute crater fill, so called breccia lens material, or they might be part of the crater wall. If they are part of the crater wall, the cataclastic breccia (Breccia 1) may have formed mostly in situ, during the compression stage. The suevitic breccia (Breccia 2) could be some kind of intrusion-like sill, injected into fractures during the excavation stage of impact crater formation, and the lithic breccia might have formed in a similar manner to the suevitic breccia (Breccia 2).

**Keywords:** Hummeln, the Hummeln structure, impact breccias, impactite classification, shock metamorphism, planar deformation features, impact craters, planar fractures, flow features, impact structures

**Supervisor(s):** Sanna Alwmark

**Subject:** Bedrock geology

*Ludvig Svensson, Department of Geology, Lund University, Sölvegatan 12, SE-223 62 Lund, Sweden. E-mail: ludvig_dino@hotmail.com*

# Sammanfattning

LUDVIG SVENSSON

Svensson, L., 2024: Ekon av nedslag: En petrografisk analys och klassificering av nedslags breccior från Hummeln, Sverige. *Examensarbete i geologi vid Lunds universitet*, Nr. 687, 25 sid. 15 hp.

**Sammanfattning:** Hummelnstrukturen är en nyligen bekräftad nedslagskrater som ligger i nordöstra delen av Småland (57.37347°N 16.25084°Ö). Eftersom den relativt nyligen bekräftades vara en nedslagskrater så finns det inte mycket detaljerade petrografiska studier var det gäller chockmetamorfos och chockmetamorfa strukturer i Hummeln-1 borrkärnan, den enda borrkärnan som finns från kratern. Borrkärnan är totalt 164,25 meter djup, mätt från sjöns yta. Den här studien beskriver och klassificerar tre breccior från de lägre delarna av borrkärnan samt diskuterar deras relation till kraterns bildning. Tre tunnslip från dessa breccior analyserades med polarisationsmikroskop, varav två dessutom med svepelektronmikroskop (SEM). I ordning uppifrån och ner, är den första en monomikt kataklastisk impaktbreccia (Breccia 1), som ligger mellan 159,14 och 160,45 meter. Den andra bergarten (Breccia 2) är en polymikt suevitisk impaktbreccia (160,45–160,75 m) som innehåller chockmetamorfa strukturer i kvartskorn i form av *planar fractures* (PFs) och *planar deformation features* (PDFs). Den tredje bergarten (Breccia 3) är en polymikt litisk impaktbreccia som ligger mellan 160,75 och 161,4 meter. Dessa breccior kan ha bildats antingen genom en process som kallas ”slumping” under modifikationsstadiet av kraterbildningen, och därför utgöra delar av kraterfyllnad, så kallad breccialins, eller så kan de utgöra en del av kraterväggen. Om de utgör en del av kraterväggen så har den kataklastiska breccian (Breccia 1) bildats för det mesta in situ under kompressionsstadiet av kraterbildningen. Den suevitiska breccian (Breccia 2) kan ha bildats som en intrusionsliknande *sill*, som injicerats i sprickorna under utgrävningsstadiet av kraterbildningen, och den litiska breccian (Breccia 3) kan a bildats på ett liknande sätt som den suevitiska breccian.

**Nyckelord:** Hummeln, Hummelnstrukturen, nedslagsbreccior, impactite klassifikation, planar deformation features, nedslags kratrar, planar fractures, flödes texturer, nedslagsstrukturer

**Handledare**: Sanna Alwmark

**Ämnesinriktning**: Berggrundsgeologi

*Ludvig Svensson, Geologiska institutionen, Lunds universitet, Sölvegatan 12, 223 62 Lund, Sverige. E-post: ludvig_dino@hotmail.com*

# 1 Introduction

Understanding meteorite impacts and the process of impact cratering has become increasingly popular in the geoscientific community. Impact cratering was long regarded as an insignificant geological process, but in recent times that view has changed dramatically with the realization that impact craters are more common than previously thought (Osinski et al., 2022). This realization also came with the understanding that impact events can cause massive amounts of destruction on even a geological scale. Meteorite impacts, when energetic enough, are extreme events that push target rocks to and beyond their limits, and form large scale deformation structures of the crust known as impact craters. Because of the extreme pressure-temperature conditions during impact crater formation, these structures are interesting from a geological and scientific perspective and act as natural laboratories for high pressure environments (French, 1998).

However, in many places the shock metamorphic features used as unambigous evidence of an impact event has since long been eroded. Studying craters might lead to the discovery of new features that can be used as evidence for an impact event which could help identifying new craters (Kenkmann, 2003; Kenkmann et al., 2014).

One large-scale structure that was recently added to the list of confirmed impact structures is the Hummeln structure (Alwmark et al., 2015) in Småland, southern Sweden. Studying craters like this one here on Earth can help us better understand both the impact events, how materials respond to these intense events, and understand other celestial bodies like the Moon and Mars (Alwmark et al., 2015).

## 1.1 Background on the Hummeln structure

The Hummeln structure is an impact structure located in the northeastern parts of the province of Småland in Sweden (57.37347°N 16.25084°Ö; Fig. 1). The structure is a roughly 1.2 km wide depression situated inside of lake Hummeln (Alwmark et al., 2015; Lindström et al., 1999). The bedrock in the area consists mainly of porphyric granite belonging to the Trans-Scandinavian Igneous Belt (TIB) (Fig. 1) (Lindström et al., 1999). The Hummeln structure's origin has been a heated topic of debate since the late 19th century when it was first discovered (Alwmark et al., 2015). The two most prominent hypotheses were explosive vulcanism and an impact event (Lindström et al., 1999). The structure was long listed as a possible impact crater in Swedish geological literature and Lindström et al (1999) provided proof of the existence of Cambrian and Ordovician sedimentary rock deposits inside the depression by drilling to 164.24 m below the lakes surface. At the drillsite, the sedimentary rock deposits were found 17.1 meters under the lake surface under a 3.1 meter layer of boulder till, deposited during the Pleistocene. Lindström et al (1999) argued that the Cambrian and Ordovician sedimentary rock deposits did not seem to have been deposited inside a crater originally, which would mean that the sediments had already been deposited when the meteorite struck. With this in mind the possible impact was dated to ~470 Ma using biostratigraphy (Lindström et al., 1999). No impact diagnostic criteria was discovered (Lindström et al., 1999).

Only one drilling was done in the structure, so only one drillcore (the Hummeln-1 drill core) exists, making it a fairly unexplored crater (Fig. 1). The drilling had to stop due to economic and technical reasons. It stopped at a point were it had reached a few meters into a unit of brecciated crystaline bedrock located between 157.2 and 164.25 meters, proposed to be part of the crater fill by Lindström et al. (1999). Above this granitic unit is a Cambrian sandstone, described as containing soft sediment deformation by Lindström et al. (1999).

The final proof of the structure's origin came in 2015 in the form of planar deformation features (PDFs) in quartz, discovered by Alwmark et al (2015). PDFs are microscopic shock metamorphic features that can only form during impact events. They were found in thin sections made from the core and a boulder taken from the southern lake shore (Alwmark et al., 2015).

The purpose of this report is to make a petrographic description of one of the lower parts of the drillcore, mainly focusing on the brecciated granite, and to classify some of the rocks using the latest classification system for impactites by Stöffler et al. (2018). It is also to discuss how the rocks may have formed.

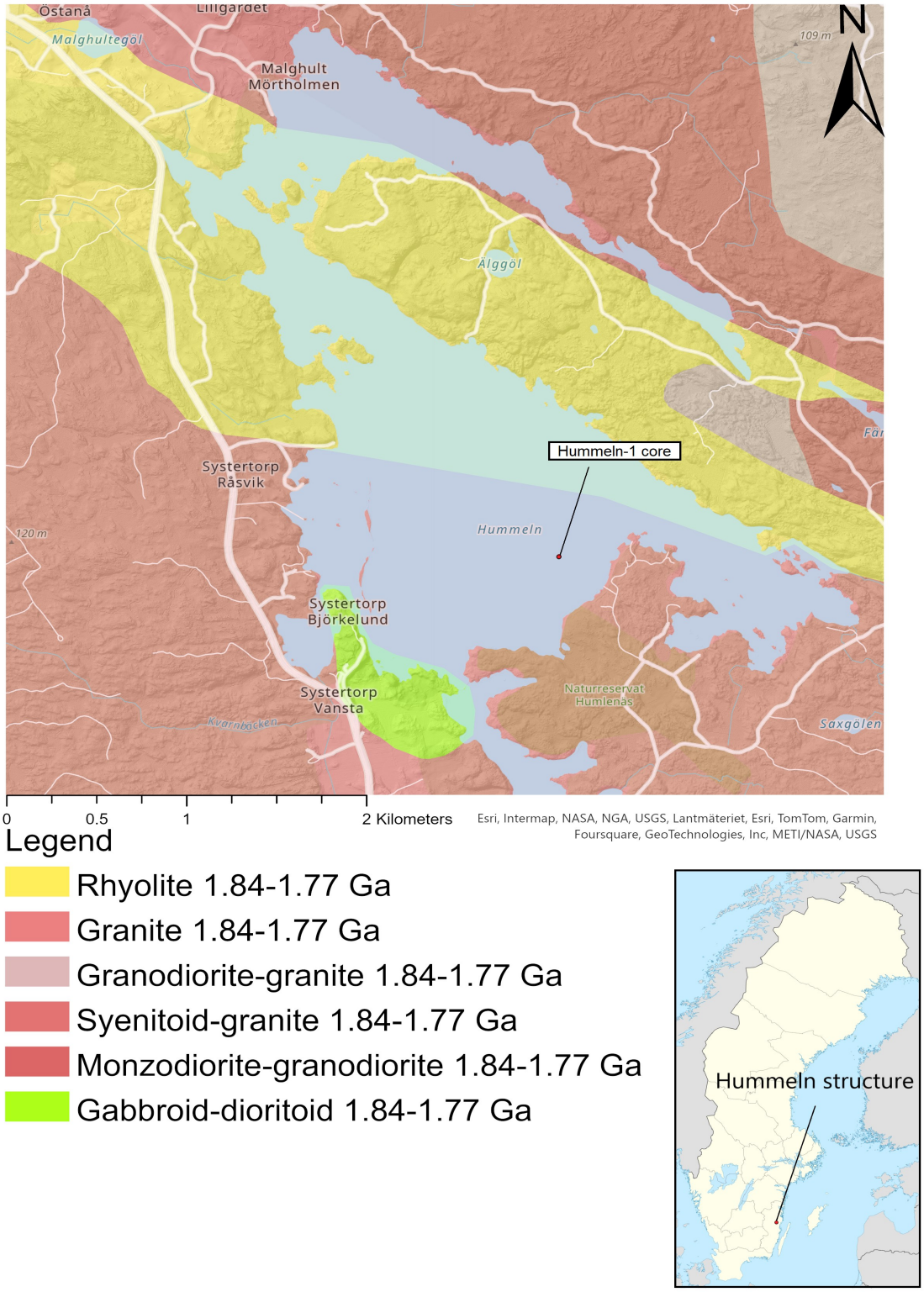


**Figure 1.** Map showing the crystalline bedrock in the lake Hummeln area, and the location of "Hummeln core 1". An overview of the location of lake Hummeln also shown in the bottom right. The bedrock map was created with the help of the map generator at the Swedish Geological Survey (SGUs) website (www.sgu.se). Legend according to SGU. The map was created in ArcGIS. Mapdata ©SGU ©Lantmäteriet.

## 1.2 Formation of impact craters

Hypervelocity impact crater formation can be divided into three stages (Collins et al., 2012) (Fig. 2).

The first stage, the compression stage, is initiated as soon as a meteorite hits the Earth's surface. Because of the meteorite's high velocity and mass, it carries immense kinetic energy which is almost instantly transferred into the target in the form of shockwaves and heat (French, 1998). These shockwaves propagate through the sediments and rocks that comprise the target lithologies. Shock compression leads to shock metamorphism and melting of the target (French, 1998). The shockwaves are also reflected back into the projectile and together with the stored elastic energy will eventually cause the meteorite to virtually completely melt and vaporize (Dypvik et al., 2010; French, 1998). Pressures that the target rock are subjected to during this stage varies depending on the distance from the centre of impact (Stöffler et al., 2018).The shockwaves propagating through the target lose their energy quickly due to dampening, one form of which is the shock waves spreading over a larger and larger volume, lowering the energy density. Some of the energy is also lost due to heating, deformation and acceleration. The loss of energy is dependent on the material; in porous rocks the shock wave loses their energy and magnitude faster than in less porous rocks (French, 1998; Kenkmann et al., 2014).

The compression stage quickly transitions into the excavation stage, where rock and sediments undergo a complex stage of fracturing, excavation of the pulverised rock, and flow outwards from the epicentre of the impact. This leads to a bowl-shaped crater rim forming, called a transient crater(Fig. 2) (French, 1998). The transient crater has a depth-to-diameter ratio of roughly 1 to 3 (Kenkmann et al., 2013).

The excavation stage ends when there is no energy left to eject material, and the crater enters a stage of gravitational settling called the modification stage (French, 1998). During this stage the rim "slumps" and collapses into the crater forming crater fill deposits together with the other displaced materials in the crater (French, 1998). The modification stage can be defined as ending when "things stop falling" (French, 1998). This can take a short time (<1 min) in a small crater, but up to a few minutes with a large craters (French, 1998). The time it takes is also affected by things like if the impact happened on land or in water. Water will flow back into the empty space created by the meteorite taking sediments and rock with it if it impacted into water (Dypvik et al., 2010). The modification stage also leads to the crater diameter increasing due to the collapsing of the rim which leads to the true depth-to-diameter ratio of 0.28 in simple craters and even less in larger craters (Kenkmann et al., 2013).

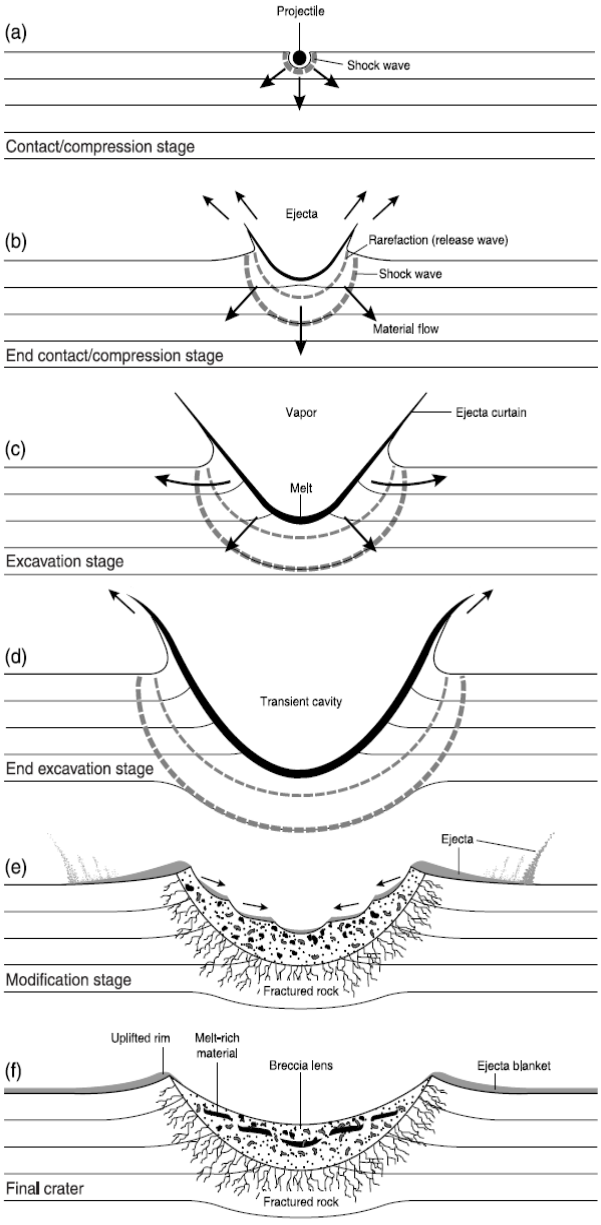


**Figure 2.** Schematic illustration of the three stages of crater formation for a simple impact crater taken from the book "Traces of catastrophe" by Bevan M. French (French, 1998). (a) and (b) shows when the projectile first hits the target and compresses it, called the compression stage. (c) and (d) shows the excavation stage where material is being pushed out of the crater as ejecta. (e) shows the last stage, the modification stage, where the crater rim is collapsing, and materials are falling back into the crater, filling it. (f) shows the final crater and a simple representation of where different impactites will end up.

After the modification stage the final crater has formed. Craters can be categorized into three types. They are the simple craters, complex craters, and a multiring basins, depending on the size of the meteorite and subsequently the final crater diameter. On Earth, if the meteorite is massive enough to form a big crater (>2-4 km, depending on target rock characteristics), the crater might undergo a stage of central uplift and form a complex crater, where major brittle deformation and brecciation happens. A smaller size impact results in the formation of a simple crater, with minor to no central uplift (French, 1998). This report focuses mainly on simple craters.

## 1.3 Shock metamorphic features in quartz

When shockwaves propagate through the target, they generate an array of different shock metamorphic features alongside fracturing in rocks and minerals, some of which can be used as unambiguous evidence of impact. This is due to the high-pressure shockwaves compressing the materials, which leads to inelastic damage in the form of both brittle and plastic deformation, but also melting and vaporisation closer to the centre of impact, which could be considered something beyond the brittle and plastic regime (Fossen, 2010; Poelchau & Kenkmann, 2011). The features produced include shatter cones, which are the only unequivocal evidence of impact that are macroscopic, planar fractures (PFs), diaplectic glass, high-pressure mineral polymorphs, and planar deformation features (PDFs) (Kenkmann et al., 2014; Poelchau & Kenkmann, 2011).

Shock metamorphic features of highest relevance to the present study are PDFs and PFs in quartz, because quartz can survive for very long periods of geologic time due to its stable nature. The features can also be seen through regular polarizing microscopes and look like sets of parallel lines. This is because they form as sets of parallel planes inside individual mineral grains.

PFs are a type of brittle feature that form at pressures between 5-8 GPa. They are open fractures 5-10 µm wide occurring in parallel sets, where each fracture typically has a spacing of around 15-20 µm. PF-like features can form during volcanic eruptions so they cannot always be used as a definite proof of an impact event. However, in multiple orientations in the same grain, and if occurring in many grains in a sample, PFs can be used as evidence of impact (French, 1998). Kenkmann et al (2011) suggested that PFs containing feather features should be added to the list of primary criteria for identifying impact craters.

PDFs in quartz form under pressures that only arise during impact events and are a type of plastic deformation. Explaining exactly how they form is beyond the scope of this paper, but they are amorphous lamellae oriented along specific crystallographic orientations which can be measured with a universal stage (U-stage). They are thinner than PFs, <2-3 µm and occur in sets where individual lamellae are more closely spaced than PFs, at around 2-10 µm. PDFs in quartz have been the go-to feature to determine the impact origin of structures on Earth (French, 1998). PDFs form from 5-10 GPa to about 35 GPa (French, 1998; Kenkmann et al., 2014).

## 1.4 Impactites

During all three stages of crater formation, several different rock types form, with varying composition and lithology. Examples include breccias and impact melt rock.

All these rocks can be categorized with an all-encompassing name “impactites” (French, 1998). Impactites can be grouped into two types depending on their location in relation to the crater, “proximal impactites” and “distal impactites” (Fig. 3 & 4) (Stöffler et al., 2018).

Distal impactites are defined as the materials that got thrown out of the crater during the excavation stage and landed outside something known as the crater’s ejecta blanket. The ejecta blanket is a proximal impactite deposit composed of ejecta, that only exists around a crater, usually within <5 crater radiuses from the centre of the crater. This means the definition for distal impactites are materials that have been displaced to a distance >5 crater radii, including up to a global distribution. The ejecta blanket becomes thinner the further away you get from the crater, and it forms during the ejection stage and the modification stage. Distal impactites are also often called airfall beds (Fig. 3) (French, 1998; Stöffler & Grieve, 2007; Stöffler et al., 2018).

Proximal impactites are defined as impactites that occur inside the outer boundary of the continuous ejecta blanket, i.e. they are defined as being within 5 crater radii of the crater (Stöffler & Grieve, 2007). Proximal impactites are distributed inside impact craters in different crater sections, one being the ejecta blanket, others include the crater floor, and the crater fill deposits (Fig. 3) (Stöffler et al., 2018). The crater fill deposits are a mix of impact melt rocks, and breccias that got mixed during the modification stage, and the fractured yet largely in-place rocks of the crater floor. Impact melt rocks are mainly produced during the compression stage and the ejection stage. They can form as a thick coherent layer in larger craters, due to the initial shock waves carrying so much energy (Fig. 2) (French, 1998; Stöffler et al., 2018). According to Osinski et al. (2022) melting and vaporisation occurs due to the shock waves forming rarefaction waves which decompresses the materials, this causes energy loss in the form of heat. What essentially happens is very fast adiabatic decompression which leads to melting and vaporisation (Kenkmann et al., 2014).

The breccias that form during an impact event include cataclastic breccias, suevitic breccias, and lithic breccias. Cataclastic breccias are monomict parautochthonous breccias, meaning they are something in between autochthonous (rocks that remains in situ) and allochthonous (moved away from its point of origin). Lithic breccias are usually polymict unless it is a single-lithology target, they are allochthonous and contain shocked and unshocked mineral grains. Lithic breccias can be found in the crater fill deposits, in the crater rim. They can also form as dikes in the crater floors and walls. Suevitic breccias (described in more detail below, section 1.4.1) are polymict breccias that contain melt particles and lithic fragments. Suevitic breccias are allochthonous and are usually found as

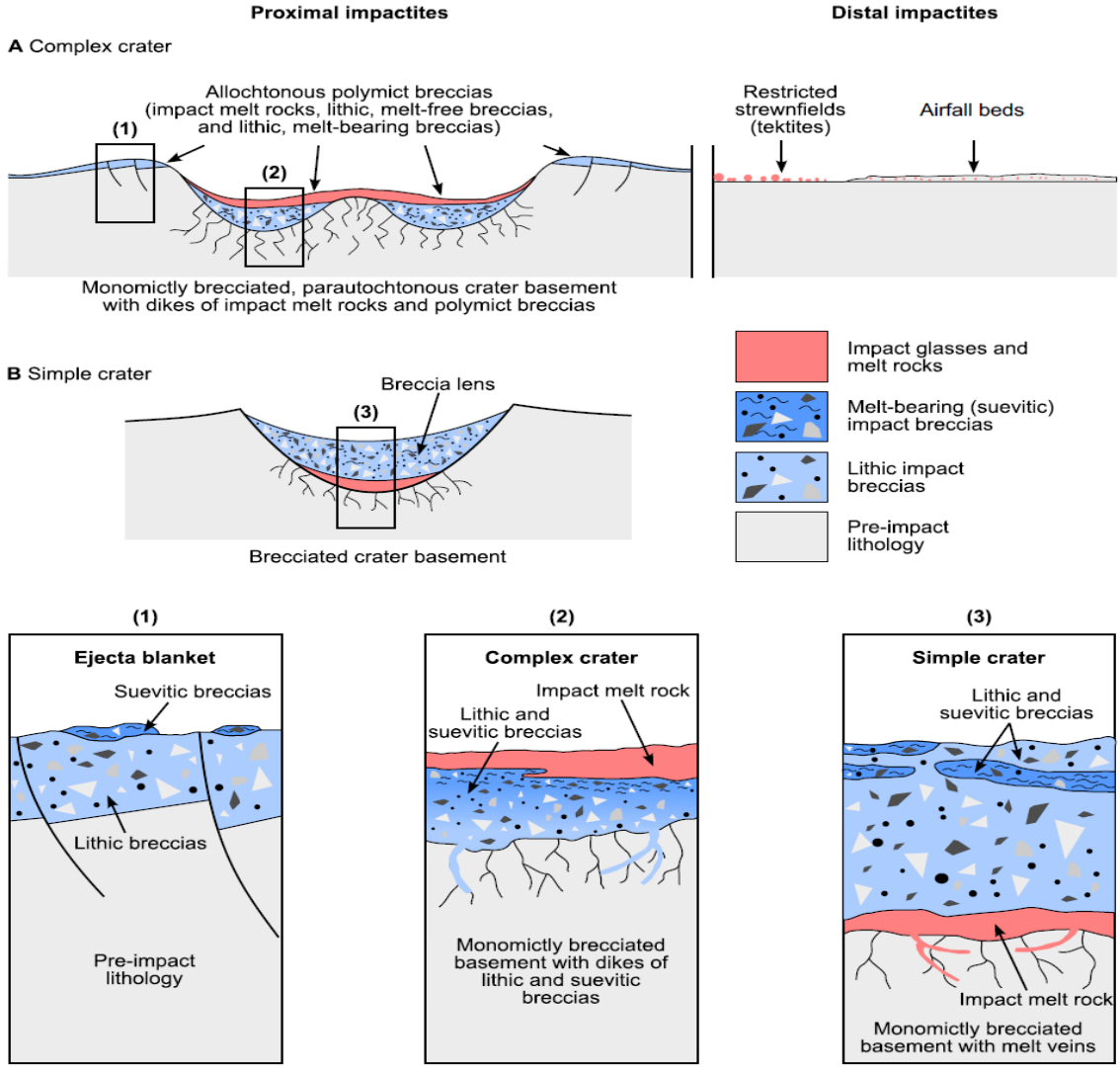


**Figure 3.** Illustration showing the location of different impactites in simple and complex impact craters. Illustration is based on the situation on Earth. Illustration taken from (Stöffler et al., 2018).

lenses inside the crater fill deposits but can also occur as part of the crater rim, or form as dikes in brecciated target rocks (Fig. 3 & 4). These dikes should not be confused with magmatic intrusions, despite the same terminology. These intrusions form in the walls and floors of craters, usually during the ejection stage or the modification stage through materials being injected into fractures (Lambert, 1981; Stöffler & Grieve, 2007; Stöffler et al., 2018).

### 1.4.1 Suevite and the characteristics of suevitic materials

Suevitic materials are impactites that contain glasses that have formed due to shock-induced melting. They are often mixed with fractured and fragmented materials, combined into a breccia (suevitic breccia; Stöffler et al., 2018). The glass usually forms particles inside the matrix, and can have diverse shapes, the glass particles are often referred to as melt particles or just melt. Suevitic breccias are therefor also alternatively referred to as melt-bearing breccias (Engelhardt, 1972; Stöffler & Grieve, 2007). The melt particles can occur in their vitric state or they can be devitrified, this may depend on the differing cooling rates during the crystallisation process or if they were altered afterwards due to hydrothermal processes. When there is water involved the melt might crystalize faster and form a more vitric state, but they can also react with hydrothermal water and form clay minerals, this can also happen with colder water long after impact (Engelhardt, 1972; Muttik et al., 2010; Stöffler & Grieve, 2007). According to Osinski et al. (2022) the line between lithic and suevitic impact breccia can be hard to define, as they may occur on a continuum. This is due to them having the exact same characteristics except for the presence of melt particles in the suevitic breccia. Another thing that complicates things is if the matrix itself has undergone melting in larger parts, then the rock is instead classified as an impact melt rock (Kenkmann et al., 2014).

# 2 Method

In this report three thin sections from three breccias (Breccia 1, 2 and 3), from the Hummeln-1 core were analysed using polarizing microscopy to classify them using the latest classification system by Stöffler et al., (2018) (Fig. 4) as well as describing the breccias petrographically. Two of the thin sections (160.36 & 160.68) were analysed with SEM.

The SEM analysis mainly focused on looking at the thin sections with back scatter electron imaging (BSE) and analysing their matrix texturally to determine the nature of the matrix and for presence of fine-grained materials with flow features. These can be used as evidence for melt components (French, 1998). One such identified feature with flow-texture was also analysed for bulk composition. Evidence of cataclastic fragmentation was also studied but mainly in thin section 160.36. The three breccias come from a granitic breccia unit from the lower part of the core and were also analysed and described macroscopically (Fig. 5).

# 3 Results

The images from the investigated sections of the Hummeln-1 drillcore shows three main lithologies (Fig. 5). The first breccia (Breccia 1) is a clast supported breccia containing granitic fragments, located roughly between 159.14 and 160.55 meters and has a dark green matrix (Fig. 5). The lithic fragments are mainly composed of dark red and salmon-pink potassium feldspar and quartz (Fig. 5 & 6). The fragments range in size from less than one cm up to a few centimeters and are very angular.

The second breccia (Breccia 2) located between 160.55 and 160.75m differs from the first (Fig 5.). This rock constitutes a breccia with flow features and few lithic fragments. The lithic fragments are mainly comprised of the same minerals as the lithic fragments in the first rock type, but the potassium feldspar is more orange in colour and quartz grains are more common (Fig. 5). The fragments are also generally a maximum of one centimeter in size and are sitting in a fine-

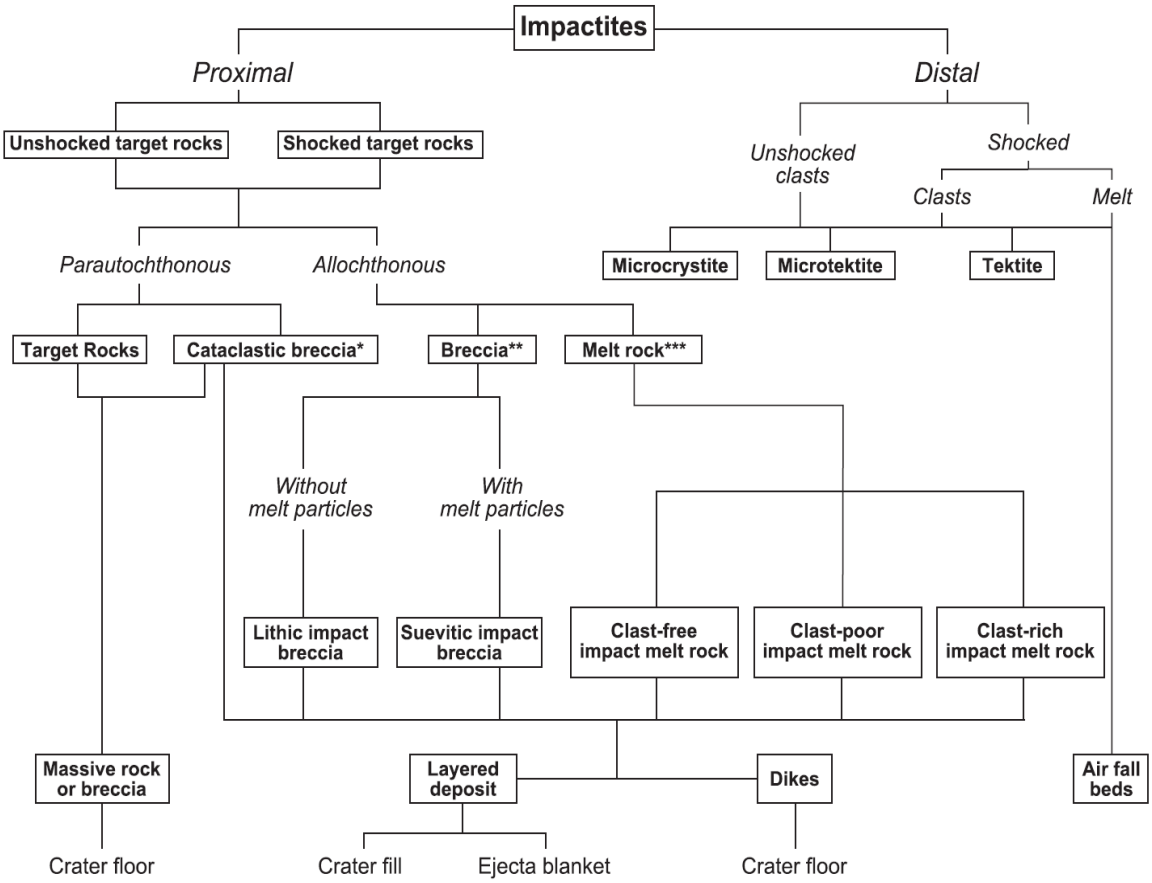


**Figure 4.** Classification system for impactites used in this report from Stöffler et al. (2018).

grained green matrix (Fig. 5 & 6).

The third breccia (Breccia 3) is located between 160.75 and roughly 161.4 meters and is a polymict breccia that does not seem to contain any flow features (Fig. 5). It contains two types of granitic fragments, one is more dark red and angular of sizes ranging from <1 to ~7 cm. The other more salmon pink, smaller ( <1-~2cm), and more rounded. There are also two types of green angular fragments, one that contain potassium feldspar, the other only plagioclase (Fig. 5).

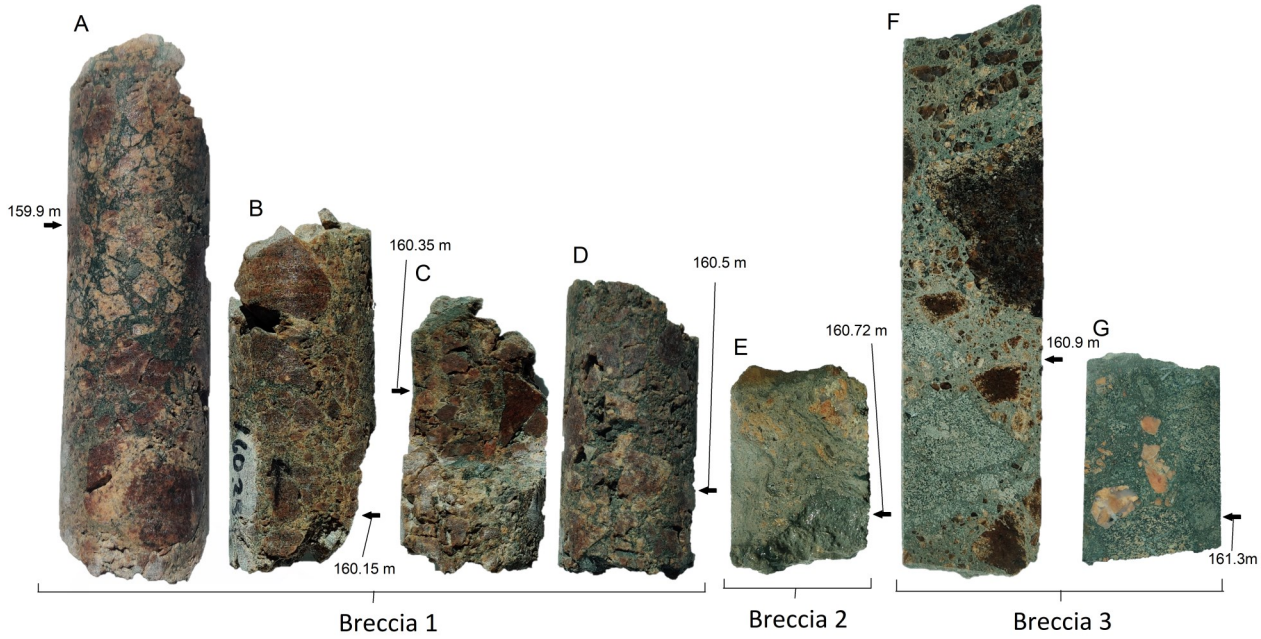


**Figure 5.** Photographs of parts of the drill core belonging to Breccia 1, Breccia 2 and Breccia 3. The diameter of the drill core is 46 mm. **A**, **B**, **C** and **D** were coated with water. Arrows denote location in meters below the lake surface. The pieces are arranged so that up in the image is up stratigraphically. **A** is a clast-supported cataclastic breccia. The clasts mainly consist of potassium feldspar and quartz, and the matrix has a dark green colour. **B** and **C** represent the same lithology as A. **C** is the sample from which thin section 160.36 was produced (Fig. 6). **D** contains slightly more matrix but is generally the same lithology as **A**, **B** and **C**. The lithology of **E** is a matrix-supported polymict breccia with a green matrix containing flow features. The matrix also contains (<1 mm) round quartz grains, also seen in Fig. 6. The lithic fragments in this breccia are composed of potassium feldspar and quartz. The feldspar is orange in colour which suggests a different origin from that in the breccia above. **E** is the location from which thin section "160.68" was produced (Fig. 6). **F** is a polymictic breccia that contains lithic fragments similar to those in **A**, **B**, **C** and **D**, except it is matrix-supported and the matrix has a lighter green colour. From about 160.9 m down it also contains dark green lithic fragments. **G** has a similar composition to **F**. Sample **G** contains multiple lithic fragments in a green matrix. This breccia also contains salmon pink granitic fragments. Thin section "161.3 A" was made from this part of the core at 161.3 m.


**Figure 6.** Photograph of the pieces that thin section 160.36 (left) and thin section 160.68 (right) was made from.

## 3.1 Thin section 160.36

Thin section 160.36 is part of a granite rich breccia. The thin section is comprised of (>2.4 mm) granitic lithic fragments of feldspars and quartz (Fig. 7). The fragments are sitting in a fine-grained matrix (Fig. 8). The rock is clast-supported. The fragments are subangular to subrounded with no signs of shock metamorphism like PFs or PDFs. One of the granitic fragments has undergone brittle deformation and something like the early stages of cataclastic flow, as intragranular shear fractures can be seen (Fig. 8). These fractures also create something similar to bookshelf sliding which can be seen on the bottom of the fragment near the bottom of the image in Fig. 8. The matrix contains some muscovite that seem to form a band like feature seen in images C), D), E) and F) (Fig. 8). These images also show part of the matrix, which consists of very poorly sorted and angular grains of quartz and feldspars. Some parts of the matrix are too fine grained to be identified with a polarizing microscope (Fig. 8). The grains in the matrix are angular to very angular (Fig. 8).

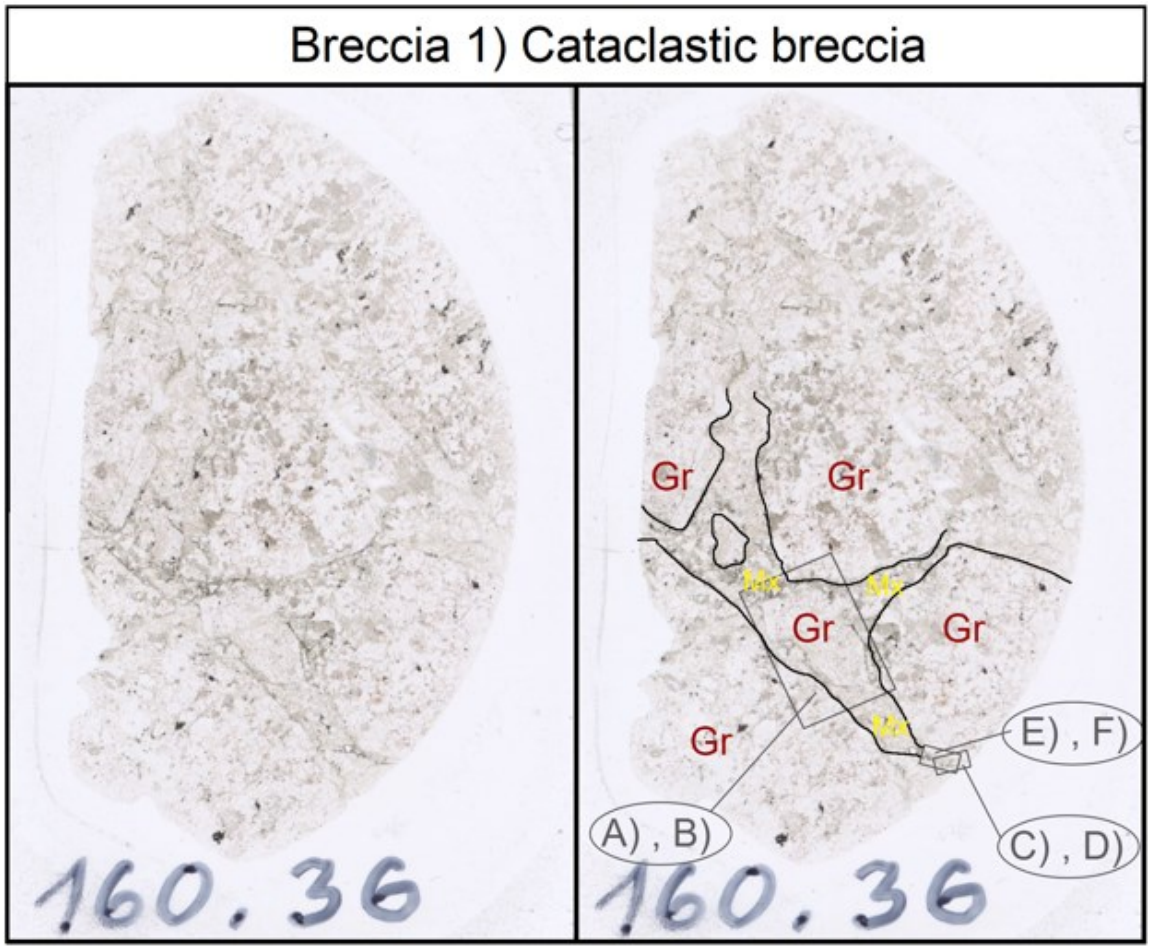


**Figure 7.** Left; scanned thin section "160.36" in plain polarized light (PPL). Right; an edited image with rectangles showing where the images in "Figure 7" are taken. The black lines outline the borders of the lithic fragments. Red labels "Gr" denotes granitic lithic fragments and yellow labels "Mx" denote the matrix.

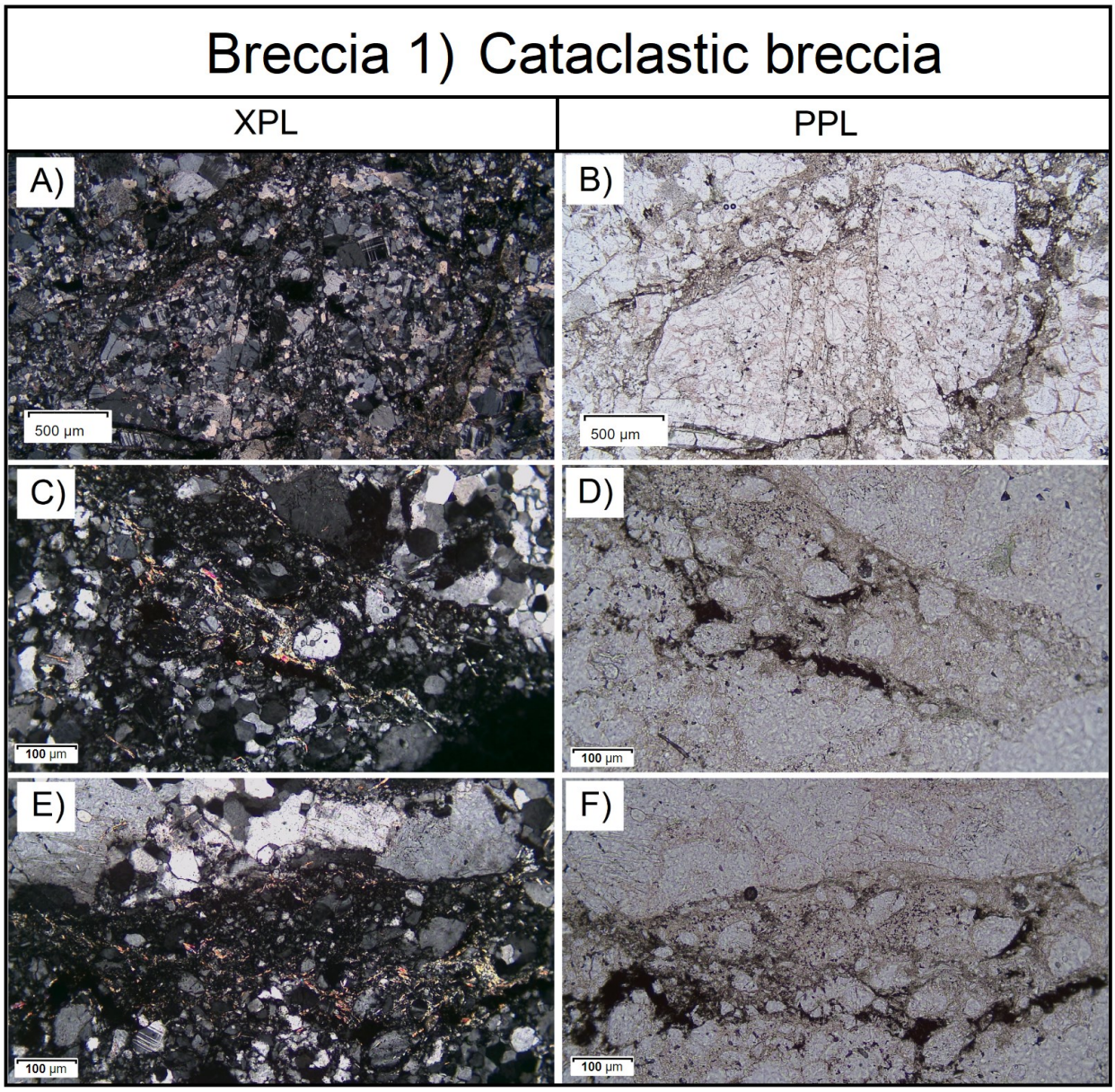


**Figure 8.** Photomicrographs of thin section 160.36 shown in XPL (left) and in PPL (right). A) A deformed lithic fragment containing feldspars like plagioclase and microcline (~60-70%) the fragment also contains quartz (~ 25-35%). The fragment has a zone of intragranular shear fractures in the central part of the sample, easier seen in PPL in image B). Images C), D), E) and F), shows areas of the matrix with lots of muscovite. They are possibly some type of cataclastic flow feature. The matrix consists mainly of quartz grains and feldspar grains, but some are too small to identify.

## 3.2 Thin section 160.68

Thin section 160.68 is a polymictic, clast-poor matrix supported breccia. The thin section is characterized by its abundance of well rounded quartz grains containing PFs and PDFs, set in a fine-grained matrix. There are also a few larger ~1-2.4 mm lithic fragments that are dominated by quartz and feldspar. The feldspar grains in these fragments usually have a perthitic texture. (Fig. 9 & 10). One of the lithic fragments contains PFs and PDFs (Fig. 10). The matrix consists of a mix of <10-100 µm quartz and feldspar fragments that vary from angular to well rounded, though some grains can be difficult to correctly identify due to their small size. The matrix also contains very fine-grained darker brown areas which seem to be fragments of some sort, they range in size from few hundred micrometres to a few millimetres.

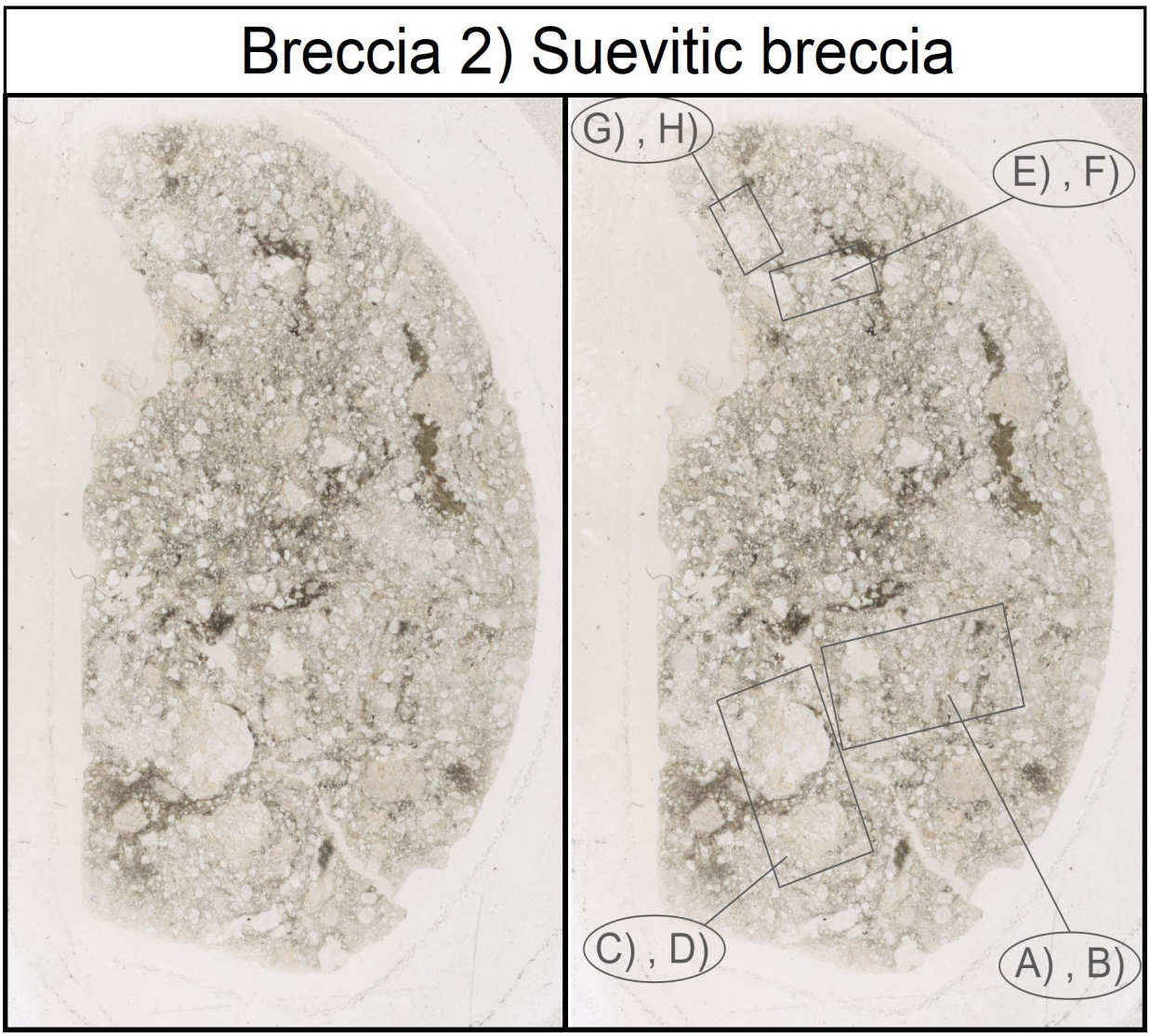


**Figure 9.** Scanned thin section 160.68 (left) and edited version (right) showing the locations of photomicrographs in Fig. 10.

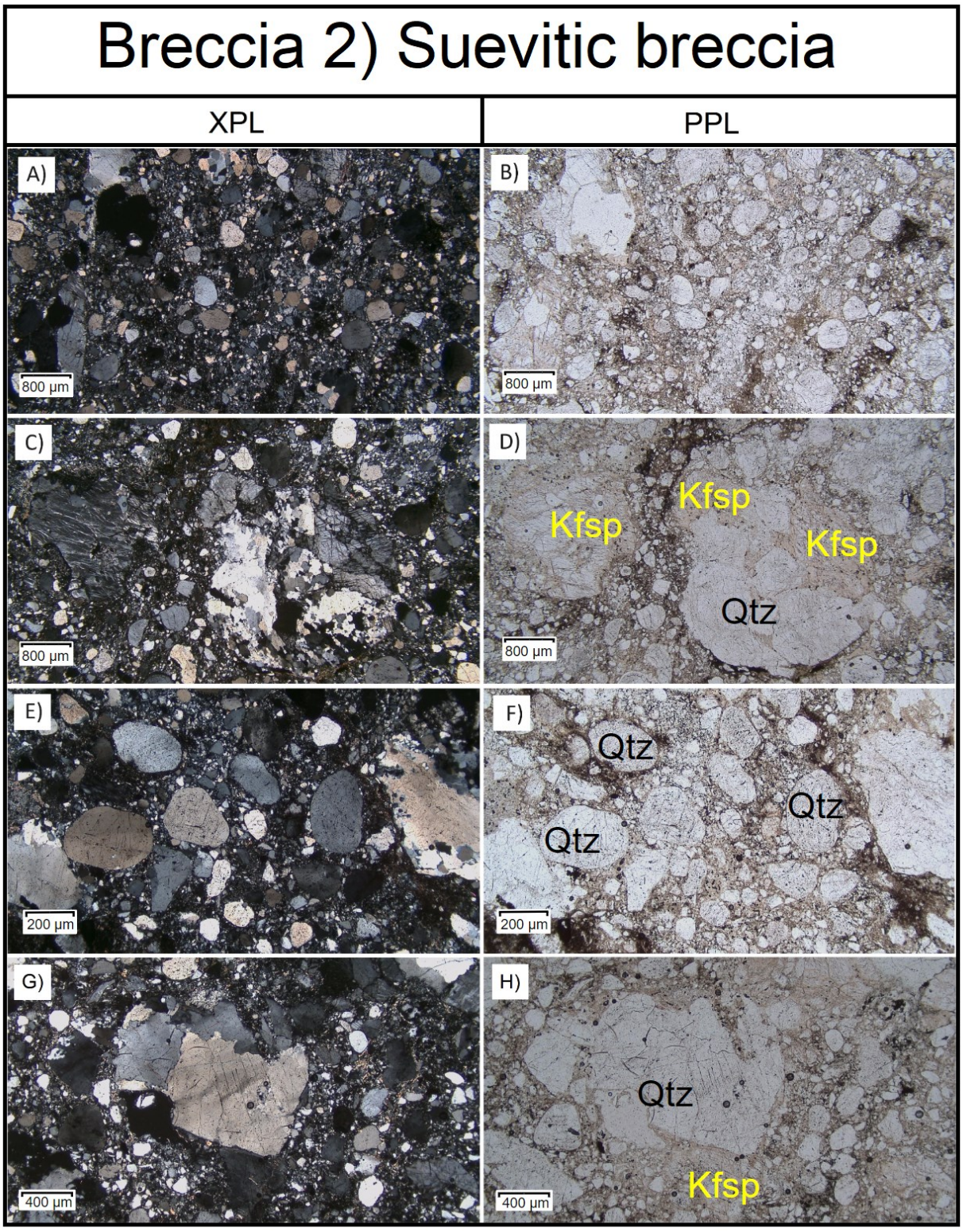


**Figure 10.** Photomicrographs of thin section 160.68 in XPL and in PPL. A) and B) shows overview images of the general composition of the thin section. It contains lots of well-rounded quartz grains and a few lithic fragments that are more angular, in a matrix of grains of varying roundness, some well rounded and some very angular. Certain areas of the matrix are very fine grained. C) and D) shows the two largest lithic fragments in this thin section. The left fragment in the image is composed of ~90% potassium feldspar with perthitic texture, and the right fragment of ~60% quartz ~40% feldspar. E) and F) is a closeup on well-rounded quartz grains containing PFs. G) and H) shows a lithic fragment composed of quartz and some potassium feldspar (Kfsp). The quartz contains PFs, parallel to these there are also much smaller lines with closer spacing.

## 3.3 Thin section 161.3A

This thin section is a matrix-supported polymict, possibly suevitic or lithic, breccia containing three types of lithic fragments in a fine-grained biotite-rich matrix. The first type of fragment is ~1-2 cm subangular and contains biotite and smaller amounts of feldspars. The second type is ~1 cm large but comprised mostly of plagioclase which has undergone sericitization. It also contains muscovite and biotite in smaller amounts (Fig. 11). The third type consists of smaller (0.2-1 mm), fragmented, grains of potassium feldspar that are very angular (Fig. 11). There is also a larger (~9 mm) rounded and less fragmented (Fig. 11) potassium-feldspar rich clast. This breccia does not show any signs of shock metamorphism. The matrix is mainly composed of biotite, but fragments of feldspars do occur.

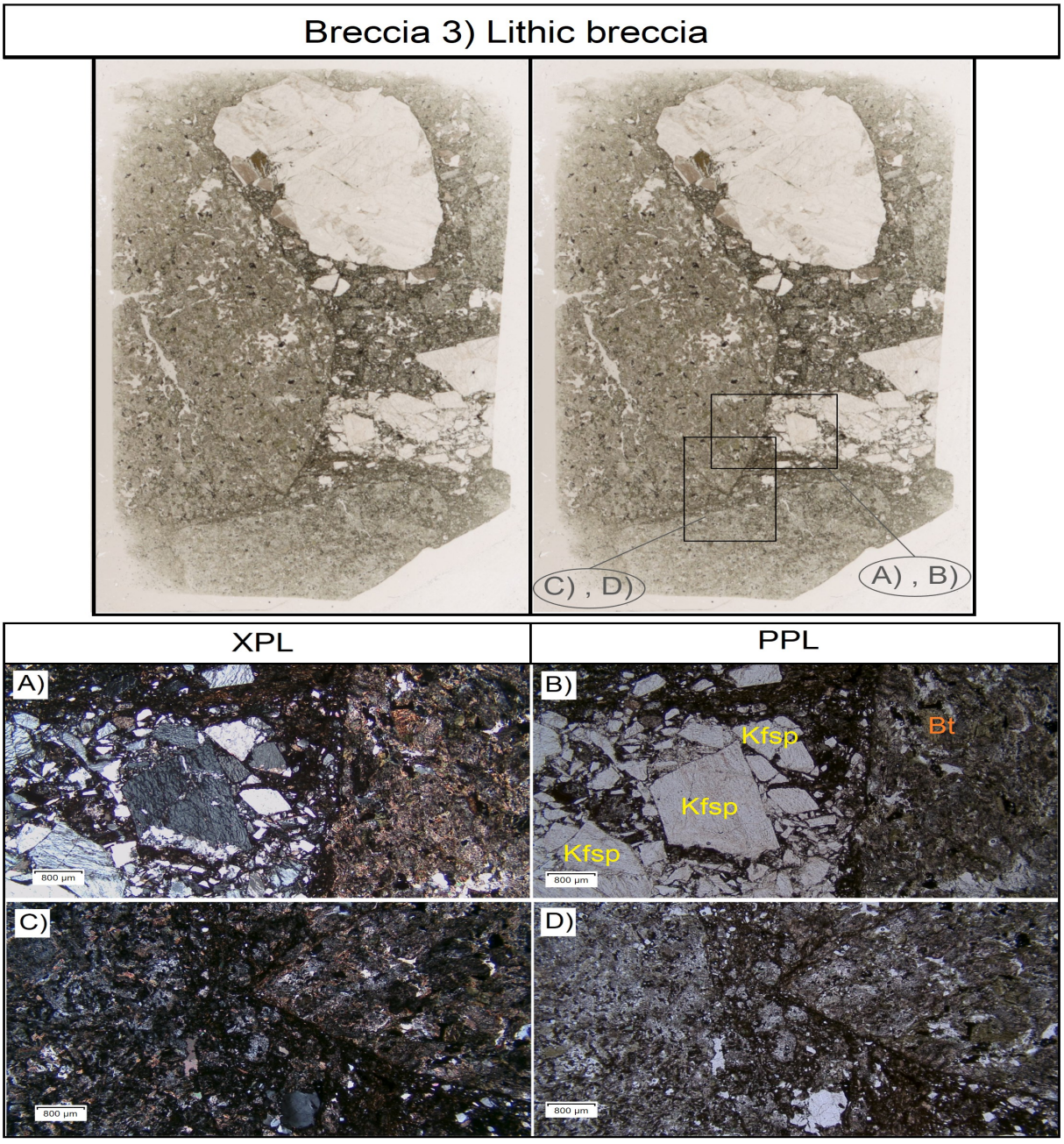


**Figure 11.** Photomicrographs of thin section 161.3A in XPL and PPL showing a lithic polymict breccia (below) and their locations in the scanned thin sections (above). A) and B) shows very angular grains of feldspars with phertitic texture marked with "Kfsp" next to a large biotite rich (~80% biotite) lithic fragment that also contains feldspar; the biotite is marked "Bt". The fragments are set in a fine-grained biotite-rich matrix without apparent flow features. C) and D) show the same large lithic fragment next to another large lithic fragment containing plagioclase that has undergone alteration to sericite. The fragment also contains some muscovite and biotite.

## 3.4 Results from SEM analysis of thin section 160.36

The SEM analysis of thin section 160.36 shows that its matrix is composed of grains that have undergone fragmentation and cataclasis. The much larger lithic fragments contain lots of fractures and in some areas, it seems to have generated material that looks similar to the matrix texturally. It also shows that there are no melt components anywhere in the matrix nor any grain boundary melts or glass fragments (Fig. 12).

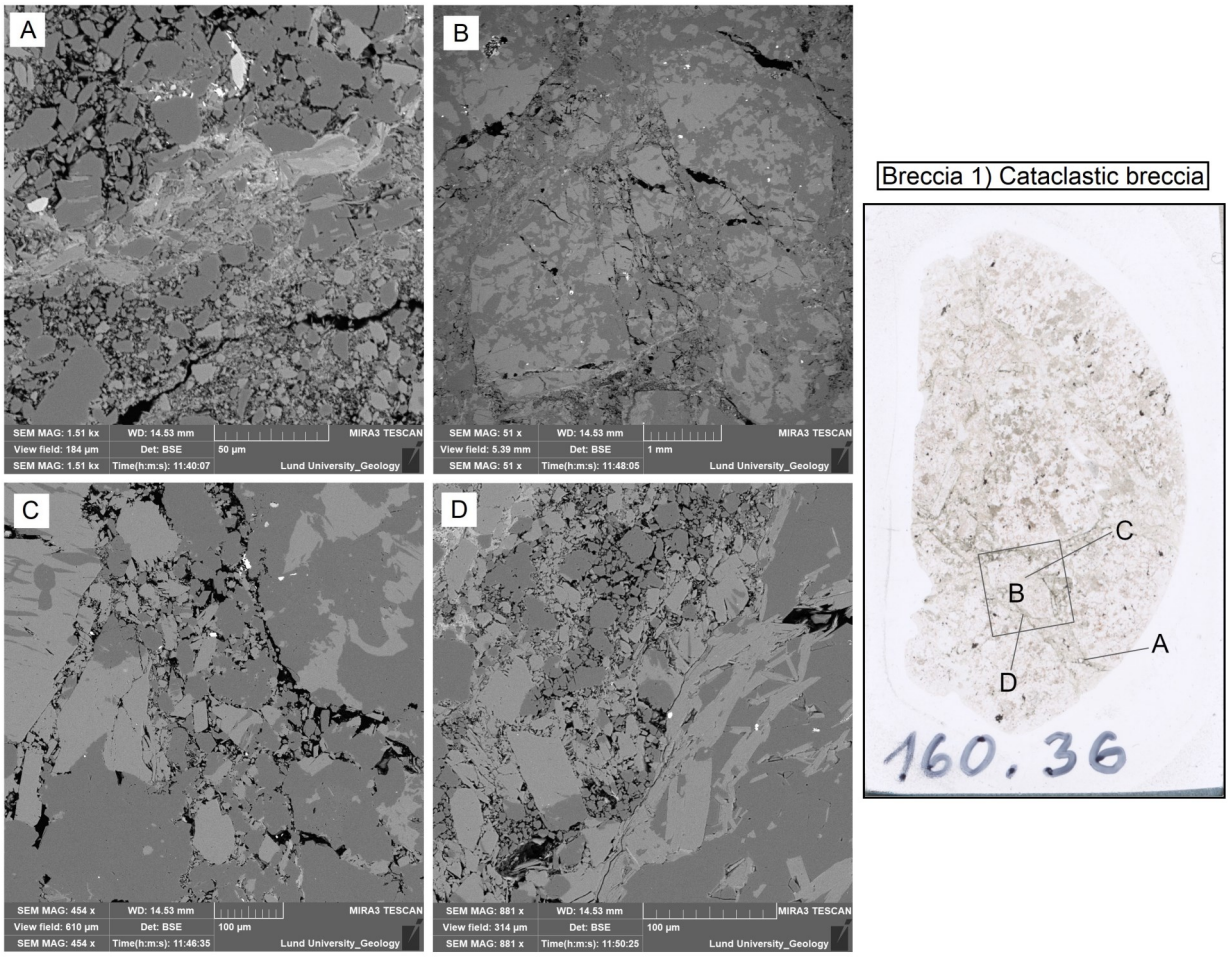


**Figure 12.** BSE images of thin section 160.36 (left), with their locations in the scanned thin section (right). A) A fine-grained matrix with angular grains of sizes ranging from ≤1 to 50 µm. Cutting across the centre of this image in roughly northeast to southwest directions is lighter coloured muscovite that is also seen in thin section 160.36 (Fig. 8). B) Overview image of the brittle deformed lithic fragment with bookshelf faulting seen in figure 8. C) Closeup of the same fragment with grains ranging in sizes from ~20 to ~100 µm. The grains are angular due to brittle fragmentation. D) Closeup of the matrix next to the fragmented grain. These fragments range in size from <10 µm to about ~60 µm. No flow features are present inside the matrix.

## 3.5 Results from SEM analysis of thin section 160.68

The SEM analysis of thin section 160.68 confirms that the darker areas of the matrix contains flow features. Compositional analysis of one of the flow features showed that it has a weight percentage of 22.03 % O, 11.48% Si, 7.28% Fe, 6.95% Al, 1.14% Mg, 0.39% Ca, 1.88% K and 0.29% Cl, which could be consistent with clay (Furquim et al., 2008; Osinski et al., 2022).

The analysis also showed that the largest lithic fragment in the thin section has a darker area next to it near one of its grain boundaries which contains flow features (Fig. 13). Parts of the matrix aside from the darker areas identified during optical microscopy consists of feldspar and quartz, some very angular and some well-rounded, ranging in sizes from <10 to 100 µm.

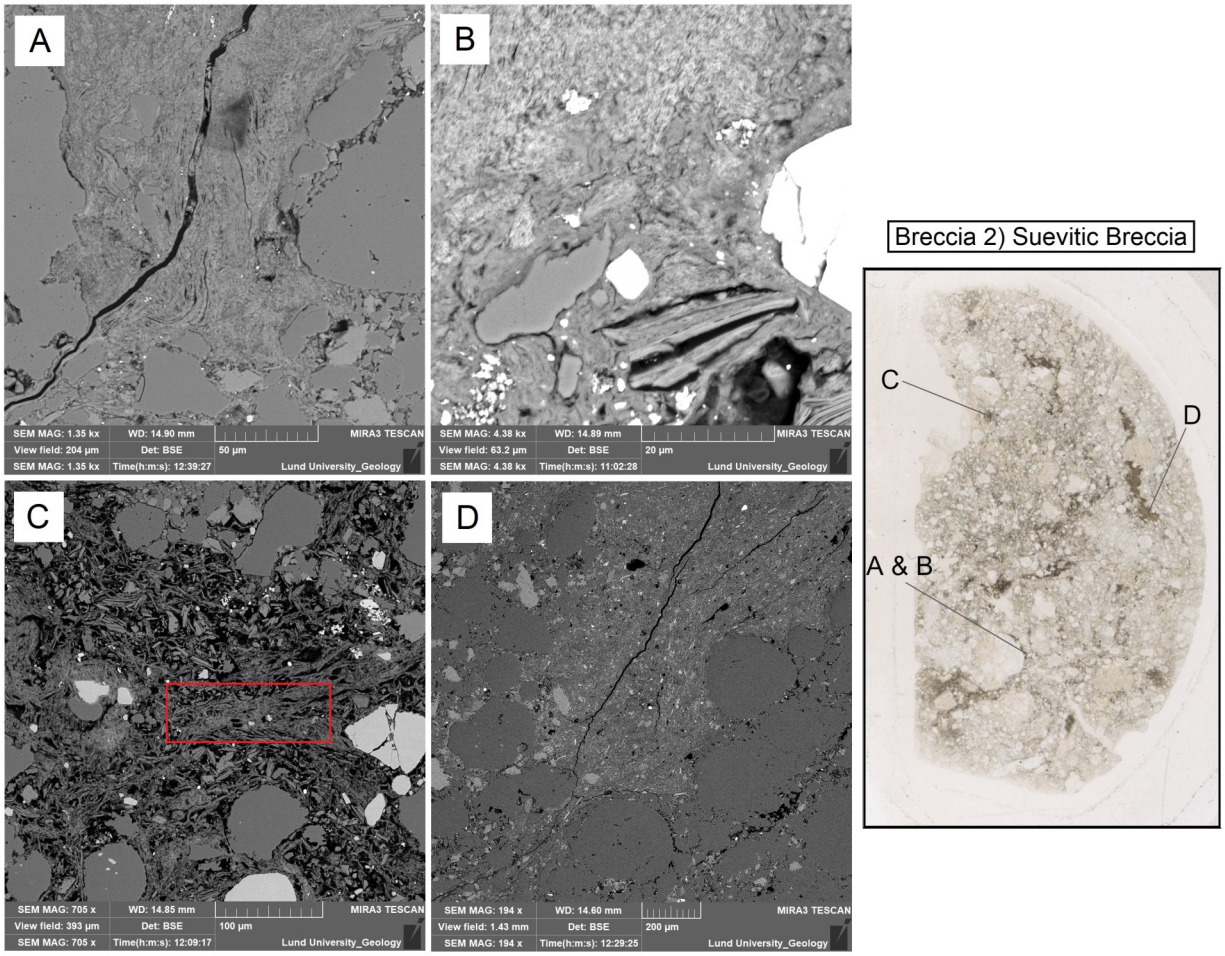


**Figure 13.** BSE images of thin section 160.68 (left) with scanned thin section showing their locations (right). A) and B) are magnifications of the darker area under the large lithic fragment in images C) and D) in Figure 10. The area contains flow features, which could be grain boundary melt. C) shows grains of varying sizes but mostly ranging from 10 to 100 µm in melt-like structures located in a brown area inside the matrix. The grains are also typical for the matrix itself. Analysis made in the rectangle, shows that the area that contains the melt-like structures might be consistent with clay. D) shows one of the fine-grained brown fragments which contains flow features. The flow features follow grain boundaries. Some of the grains are just over 200 µm and are well rounded and consist of quartz.

# 4 Discussion and classification

The results from the analysis of the drillcore shows a sharp shift in lithology at about 160.55 meters. Before this point is a granitic breccia between 159.14 and 160.55 meters (Breccia 1), after this point there is two polymictic breccias, one from 160.55 to 160.75 meters (Breccia 2) and one between 160.75 and 161.4 meters (Breccia 3), (see classification below, section 4.1, 4.2 and 4.3).

## 4.1 Breccia 1

The first (Breccia 1) between 159.14 and 160.55 meters can be described as a monomict, cataclastic breccia. This rock showed no signs of PFs or PDFs, and the matrix has undergone cataclastic flow. The SEM analysis together with the polarizing microscopy showed that the matrix probably consists of the same minerals and has the same general composition as the large lithic fragments, and that the grains have undergone fragmentation (Fig. 12). The lithic fragment in figure 8 indicates limited grain rotation and or friction-

al sliding. The muscovite seen in figure 8 has possibly formed through some type of cataclasis, maybe by the muscovite slipping along its planes during the formation of the matrix (Fig. 12).

## 4.2 Breccia 2

The breccia between 160.55 and 160.75 meters (Breccia 2) is interpreted as a matrix-supported polymict suevitic breccia. The classification is based on the presence of melt fragments, which were characterized with SEM, frequent rounded quartz grains with PFs and lithic fragments. Besides PFs one of the lithic fragments also contained much thinner bands with a closer spacing interpreted as PDFs, though they have not been measured with a u-stage.

These characteristics are consistent with the expectation that suevitic breccias contain components with shock metamorphic features (e.g., Stöffler et al., 2018; Osinski et al., 2022). The dark brown areas of the matrix are probably devitrified glass that originally formed as a result of shock induced melting (Engelhardt, 1972), this is based on the presence of flow features and that it is fine-grained. One of these dark brown areas also had a bulk composition that was in line with clay minerals, which can be used as evidence for a melt particle that has been altered by water (Fig. 13) (Osinski et al., 2022). The darker brown colours might be due to the presence of iron oxides, as iron is also present (Muttik et al., 2010; Stöffler & Grieve, 2007). Some parts of the dark brown areas contain flow features that follow grain boundaries, which could mean that the melt was mixed with the grains and had not already crystallized when the mixing happened (French, 1998). The most difficult part about the classification is that it clearly contains glass fragments that are sitting in different parts of the matrix, however, in certain areas it is harder to determine if they are fragments or if it is the matrix itself that has undergone melting. This could possibly change the classification to an impact melt rock if this turns out to be a common and widespread occurrence, though for now the classification remains a suevitic breccia. Further studies could resolve this.

## 4.3 Breccia 3

Further down in the core, from 160.75 to 161.4 meters, there is a polymict breccia (Breccia 2) containing granitic lithic fragments and three other types of lithic fragments. The matrix varies in colour from lighter green to darker green (Fig. 5 & 11). The matrix contains areas that are mostly comprised of biotite. In some places these areas look similar to something like devitrified glass, even though it does not have any well-defined flow features, this could be investigated in the future using SEM. Certain parts of the matrix are also a lot more similar to the matrix in thin section 160.36, containing more quartz and feldspar fragments. This could possibly be the more lighter green matrix seen in the core samples in Fig. 5E.

This breccia could be classified as either a polymict lithic breccia or a polymict suevitic breccia, depending on if it contains melt particles. No shock metamorphic features have been identified, although this could be due to the lack of large quartz grains (Fig. 11).

## 4.4 Possible Formation

Given that Breccia 1 does not show any signs of shock metamorphism like PFs or PDFs, the shocked lithic fragment in thin section “160.68” may have originated in a different part of the crater, perhaps closer to the center of the crater. Closer to the center of the crater the pressures from the shock waves were higher (Stöffler et al., 2018) which might have allowed shock metamorphism at greater depths even in the crystalline bedrock. That would also be in line with the fact that the potassium feldspars in the two rock types have different colors, and different quartz content, which indicates slightly different composition and possibly origin.

There are a few possible ways the granite dominated breccias in the lower part of the drill core could have formed. One is through slumping during the modification stage. In this scenario the shifting lithology as seen in the samples from the core (Fig. 5) could be explained by this section of the core being part of the layered crater fill deposits (Fig. 3 & 4; Stöffler et al., 2018). Though one thing that is hard to explain is how Breccia 1 does not show any signs of mixing, while Breccia 2 does. Breccia 2 contains many different constituents, from lithic fragments to melt to low shock pressure indicators (Stöffler et al., 2018) like rounded quartz grains with planar fractures. One possibility is that the lower unit of the drill core is the crater rim, this was discussed by Lindström et al. (1999), who postulated that the granitic unit could have been a block of shattered rim wall sitting in the crater fill deposits, that fell down during the modification stage. Although this is possible, the fact that the layers are basically horizontal sheds doubt on that idea.

Another hypothesis is that the sudden change to a suevitic breccia (Breccia 2) can be explained by it being a sill-like intrusion, like dikes, whose material originated closer to the centre of the crater. In that case the drilling might have stopped in the beginning of the crater floor or the crater wall. Following this hypothesis Breccia 1 might not have moved far from its original position when a slurry of melt rock, lithic fragments, shocked Cambrian sand grains, and possibly water, flowed into the fractures in the brecciated granite. This would have happened quickly during the compression and ejection stage. If Breccia 2 was injected in this way as a form of dike, that could have implications for how this crater formed. It could imply that this crater has more in common with a complex crater (Lambert, 1981). However, considering the crater diameter of 1.2 km, and the fact that craters become complex between at least 2 and 4 km on Earth (French, 1998), this would imply that the crater might be larger. If Breccia 2 was injected as a dike, then Breccia 3 could have formed in a similar way, though why Breccia 3 got partially mixed with similar granitic material seen in Breccia 1 while Breccia 2 did not is hard to explain. Given that the Hummeln structure currently has a diameter of 1.2 km, and it does not show any clear central uplift it is probably a simple crater. Using a depth-to-diameter ratio of 0.28 which is the ratio for simple craters (Kenkmann et al., 2013),

you would expect to reach the true crater floor at ~336 meters below the crater rim at the center of the crater. The core itself is about 143 meters from the top of the sedimentary rocks, and according to Lindström et al. (1999) the extant rim is a few tens of meters above this at the most, though it need to be clarified that this is in fact not the true rim but the crater wall. The depth of the drill core in relation to the rim puts at least some doubt on the idea that the crater floor was struck by the drilling. Though this does not consider the fact that the crater has been eroded, and the original diameter of the crater and as a result the true height of the crater rim, is unknown (Lindström et al., 1999).

Another possibility is that the crater wall was struck, this is possible considering the drilling happened closer to the edge of the crater (Lindström et al., 1999). This would likely have reduced the distance to the end of the crater fill deposits, given that the structure can be expected to have a parabolic shape (e.g., Stöffler et al., 2018) and as a result possibly rock types more in line with the crater wall or floor would have been encountered during the drilling sooner than if the drilling had been made in the center of the structure. It is also worth noting that the drilling happened on a ridge (Lindström et al., 1999). This might also have influenced how far the drill had to go before hitting the crater wall assuming the wall has been uplifted. In this case Breccia 2 and Breccia 3 could still have formed as a dike.

To confirm or disprove this hypothesis, more detailed analyses of the lowest part of the core is needed. Examples may include looking at thin section 161.3A using SEM to see if it contains melt particles, but also analyzing and mapping thin sections from other intervals of the drill core in more detail. If thin section 161.3A contains melt, it could mean that the matrix in both Breccia 2 and Breccia 3 has undergone some mixing or that they have similar points of origin.

# 6 Conclusion

This analysis provides evidence that simple craters might on some occasions have impact breccia dikes similar to those seen in complex craters given the assumption that the Hummeln structure is a simple crater. It also sheds light on the characteristics and constituents of impactites in small impact structures.

The three impactites that have been analyzed are comprised of three types of breccias that could have formed either through slumping or represent part of the crater wall. They include (from top to bottom); a monomict cataclastic breccia (Breccia 1), a polymictic suevitic breccia (Breccia 2), and a polymictic lithic breccia (Breccia 3). Only Breccia 2 shows clear evidence of shock metamorphism, in the form of PFs and PDFs and it might be a type of injection sill. This report proposes a reevaluation of the lower part of the core compared to earlier study and how these impactites may have formed.

# 7 Acknowledgements

I would like to give many thanks to my supervisor Sanna Alwmark for all the help I have received both during the writing process and during all the manual work like the polarizing microscopy. I would also like to thank Carl Alwmark for the instructions and help during the SEM analysis.

# 8 References

Alwmark, C., Ferriere, L., Holm-Alwmark, S., Ormoe, J., Leroux, H., & Sturkell, E. (2015). Impact origin for the Hummeln structure (Sweden) and its link to the Ordovician disruption of the L chondrite parent body [Article]. *Geology*, *43*(4), 279-282. https://doi.org/10.1130/g36429.1

Collins, G., Melosh, J., & Osinski, G. (2012). The Impact-Cratering Process. *Elements*, *8*, 25-30. https://doi.org/10.2113/gselements.8.1.25

Dypvik, H., Tsikalas, F., & Smelror, M. (2010). *The Mjølnir Impact Event and its Consequences: Geology and Geophysics of a Late Jurassic/Early Cretaceous Marine Impact Event*. Springer Berlin Heidelberg. https://books.google.se/books?id=4u0gS_8ee-MC

Engelhardt, W. v. (1972). Shock produced rock glasses from the Ries crater. *Contributions to Mineralogy and Petrology*, *36*(4), 265-292. https://doi.org/10.1007/BF00444336

Fossen, H. (2010). *Structural Geology*. Cambridge University Press. https://books.google.se/books?id=01PI5jhjiiQC

French, B. M. (1998). *Traces of Catastrophe: A Handbook of Shock-metamorphic Effects in Terrestrial Meteorite Impact Structures*. Lunar and Planetary Institute. https://books.google.se/books?id=LTJQAQAAIAAJ

Furquim, S., Graham, R., Barbiero, L., de Queiroz Neto, J., & Valles, V. (2008). Mineralogy and Genesis of Smectites in an Alkaline-Saline Environment of Pantanal Wetland, Brazil. *Clays and Clay Minerals*, *56*. https://doi.org/10.1346/CCMN.2008.0560511

Kenkmann, T. (2003). Dike formation, cataclastic flow, and rock fluidization during impact cratering: an example from the Upheaval Dome structure, Utah. *Earth and Planetary Science Letters*, *214*(1), 43-58. https://doi.org/https://doi.org/10.1016/S0012-821X(03)00359-5

Kenkmann, T., Collins, G., & Wünnemann, K. (2013). The Modification Stage of Crater Formation. In (pp. 60-75). https://doi.org/10.1002/9781118447307.ch5

Kenkmann, T., Poelchau, M., & Wulf, G. (2014). Structural geology of impact craters. *Journal of Structural Geology*, *62*. https://doi.org/10.1016/j.jsg.2014.01.015

Lambert, P. (1981). Breccia dikes - Geological constraints on the formation of complex craters. *Geochim. Cosmochim. Acta.*, *-1*, 59-78.

Lindström, M., Flodén, T., Grahn, Y., Hagenfeldt, S., Ormö, J., Sturkell, E. F. F., & Törnberg, R. (1999). The Lower Palaeozoic of the probable impact crater of Hummeln, Sweden [Article]. *Gff*, *121*, 243-252. https://doi.org/10.1080/11035899901213243

Muttik, N., Kirsimäe, K., & Vennemann, T. W. (2010). Stable isotope composition of smectite in

suevites at the Ries crater, Germany: Implications for hydrous alteration of impactites. *Earth and Planetary Science Letters*, *299*(1), 190-195. https://doi.org/https://doi.org/10.1016/j.epsl.2010.08.034

Osinski, G. R., Grieve, R. A. F., Ferrière, L., Losiak, A., Pickersgill, A. E., Cavosie, A. J., Hibbard, S. M., Hill, P. J. A., Bermudez, J. J., Marion, C. L., Newman, J. D., & Simpson, S. L. (2022). Impact Earth: A review of the terrestrial impact record. *Earth-Science Reviews*, *232*, 104112. https://doi.org/https://doi.org/10.1016/j.earscirev.2022.104112

Poelchau, M., & Kenkmann, T. (2011). Feather features: A low-shock-pressure indicator in quartz. *Journal of Geophysical Research*, *116*. https://doi.org/10.1029/2010JB007803

Stöffler, D., & Grieve, R. (2007). Impactites. *Metamorphic Rocks: A Classification and Glossary of Terms*, 82-92.

Stöffler, D., Hamann, C., & Metzler, K. (2018). Shock metamorphism of planetary silicate rocks and sediments: Proposal for an updated classification system (vol 53, pg 5, 2018) [Correction]. *Meteoritics & Planetary Science*, *54*(4), 946-949. https://doi.org/10.1111/maps.13246

## Tidigare skrifter i serien ”Examensarbeten i Geologi vid Lunds universitet”:

631. Svensson, David, 2022: Geofysisk och geologisk tolkning av kritskollors utbredning i Ystadsområdet. (15 hp)
632. Allison, Edward, 2022: Avsättning av Black Carbon i sediment från Odensjön, södra Sverige. (15 hp)
633. Jirdén, Elin, 2022: OSL dating of the Mesolithic site Nilsvikdalen 7, Bjorøy, Norway. (45 hp)
634. Wong, Danny, 2022: GIS-analys av effekten vid stormflod/havsnivåhöjning, Morupstrakten, Halland. (15 hp)
635. Lycke, Björn, 2022: Mikroplast i vattenavsatta sediment. (15 hp)
636. Schönherr, Lara, 2022: Grön fältspat i Varbergskomplexet. (15 hp)
637. Funck, Pontus, 2022: Granens ankomst och etablering i Skandinavien under postglacial tid. (15 hp)
638. Brotzen, Olga M., 2022: Geologiska besöksmål och geoparker som plattform för popularisering av geovetenskap. (15 hp)
639. Lodi, Giulia, 2022: A study of carbon, nitrogen, and biogenic silica concentrations in *Cyperus papyrus*, the sedge dominating the permanent swamp of the Okavango Delta, Botswana, Africa. (45 hp)
640. Nilsson, Sebastian, 2022: PFAS- En sammanfattning av ny forskning, med ett fokus på föroreningskällor, provtagning, analysmetoder och saneringsmetoder. (15 hp)
641. Jägfeldt, Hans, 2022: Molnens påverkan på jordens strålningsbalans och klimatsystem. (15 hp)
642. Sundberg, Melissa, 2022: Paleontologiska egenskaper och syreisotopsutveckling i borrkärnan Limhamn-2018: Kopplingar till klimatförändringar under yngre krita. (15 hp)
643. Bjermo, Tim, 2022: A re-investigation of hummocky moraine formed from ice sheet decay using geomorphological and sedimentological evidence in the Vomb area, southern Sweden. (45 hp)
644. Halvarsson, Ellinor, 2022: Structural investigation of ductile deformations across the Frontal Wedge south of Lake Vättern, southern Sweden. (45 hp)
645. Brakebusch, Linus, 2022: Record of the end-Triassic mass extinction in shallow marine carbonates: the Lorüns section (Austria). (45 hp)
646. Wahlquist, Per, 2023: Stratigraphy and palaeoenvironment of the early Jurassic volcaniclastic strata at Djupadalsmölla, central Skåne, Sweden. (45 hp)
647. Gebremedhin, G. Gebreselassie, 2023: U-Pb geochronology of brittle deformation using LA-ICP-MS imaging on calcite veins. (45 hp)
648. Mroczek, Robert, 2023: Petrography of impactites from the Dellen impact structure, Sweden. (45 hp)
649. Gunnarsson, Niklas, 2023: Upper Ordovician stratigraphy of the Stora Sutarve core (Gotland, Sweden) and an assessment of the Hirnantian Isotope Carbon Excursion (HICE) in high-resolution. (45 hp)
650. Cordes, Beatrix, 2023: Vilken ny kunskap ger aDNA-analyser om vegetationsutvecklingen i Nordeuropa under och efter Weichsel-istiden? (15 hp)
651. Bonnevier Wallstedt, Ida, 2023: Palaeocolour, skin anatomy and taphonomy of a soft-tissue ichthyosaur (Reptilia, Ichthyopterygia) from the Toarcian (Lower Jurassic) of Luxembourg. (45 hp)
652. Kryffin, Isidora, 2023: Exceptionally preserved fish eyes from the Eocene Fur Formation of Denmark – implications for palaeobiology, palaeoecology and taphonomy. (45 hp)
653. Andersson, Jacob, 2023: Nedslagskratrars inverkan på Mars yt-datering. En undersökning av Mars främsta yt-dateringsmetod ”Crater Counting". (15 hp)
654. Sundberg, Melissa, 2023: A study in ink – the morphology, taphonomy and phylogeny of squid-like cephalopods from the Jurassic Posidonia Shale of Germany and the first record of a loligosepiid gill. (45 hp)
655. Häggblom, Joanna, 2023: En patologisk sjölilja från silur på Gotland, Sverige. (15 hp)
656. Bergström, Tim, 2023: Hur gammal är jordens inre kärna? (15 hp)
657. Bollmark, Viveka, 2023: Ca isotope, oceanic anoxic events and the calcareous nannoplankton. (15 hp)
658. Madsen, Ariella, 2023: Polycykliska aromatiska kolväten i Hanöbuktens kustnära sediment - En sedimentologisk undersökning av vikar i närhet av pappersbruk. (15 hp)
659. Wangritthikraikul, Kannika, 2023: Holocene Environmental History of Warming Land, Northern Greenland: a study based on lake sediments. (45 hp)
660. Kurop, Anna, 2023: Reconstruction of the glacier dynamics and Holocene chronology of retreat of Helagsglaciären in Central Sweden. (45 hp)
661. Frisendahl, Kajsa, 2023: Holocene environmental history of Washington Land,

NW Greenland: a study based on lake sediments. (45 hp)

662. Ryan, Cathal, 2023: Luminescence dating of the late Quaternary loess-palaeosol sequence at Velika Vrbica, Serbia. (45 hp)
663. Lindow, Wilma, 2023: U-Pb datering av zirkon i metasediment tillhörande Stora Le-Marstrand, SV Sverige. (15 hp)
664. Bengtsson, Kaisa, 2023: Geologisk karaktärisering av den kambriska Faluddensandstenen i Östersjön och dess lämplighet för koldioxidlagring. (15 hp)
665. Granbom, Johanna, 2023: Insights into simple crater formation: The Hummeln impact structure (Småland, Sweden). (45 hp)
666. Jonsson, Axel, 2023: Datering av vulkanen Rangitoto, Nya Zeeland, genom paleomagnetiska analysmetoder. (15 hp)
667. Muller, Elsa, 2023: Response of foraminifera *Ammonia confertitesta* (T6) to ocean acidification, warming, and Deoxygenation An experimental approach. (45 hp)
668. Struzynska, Patrycja, 2023: Petrography, geochemistry, and origin of deep magmatic cumulates in the Canary Islands – the xenolith record. (45 hp)
669. Krätzer, Tobias, 2023: Artificiella torskrev i Hanöbukten: Förstudie. (15 hp)
670. Khorshidian, Farid, 2023: 3D modelling and resistivity measurements for hydrogeological assessments in the northern part of Vombsänkan. (45 hp)
671. Sundberg, Oskar, 2023: Methodology for Stored Heat “Heat In Place” (HIP) assessment of geothermal aquifers – Exemplified by a study of the Arnager Greensand in SW Scania. (45 hp)
672. Haraldsson, Emil, 2023: Kan akademin hjälpa industrin utveckla mer robusta grundvattenmodeller? En studie av moderna Svenska industriframtagna grundvattenmodeller. (15 hp)
673. Barabas, Ricky, 2024: Kan chockmetamorfos i okonventionella mineral hjälpa till att identifiera nedslagskratrar? (15 hp)
674. Nilsson, Sebastian, 2024: The glaciotectonic evolution of Ven, Sweden: insights from a comprehensive structural, sedimentological, and geomorphological analysis. (45 hp)
675. Brotzen, Olga M., 2024: A new Lagerstätte-like fossil assemblage from the early Silurian of Mösseberg, Sweden. (45 hp)
676. Eng, Simon, 2024: Precursors to the South Atlantic Anomaly - Magnetic field variations in Lake Eilandvlei, South Africa. (45 hp)
677. Husén, Simon, 2024: Structural Geological Model of the Kaunisvaara Mining District, Norrbotten, Sweden. (45 hp)
678. Hjalmarsson, Tilda, 2024: Det underkambriska problematiska fossilet *Spatangopsis* - Vad är dess verkliga affinitet? (15 hp)
679. Kuberna, Marcos, 2024: En litteraturstudie om klorparaffiner i grundvattnet och dess implikationer på hälsa och miljö. (15 hp)
680. Persson, Viktor, 2024: Litteraturstudie: HIMU ursprung och framtid. (15 hp)
681. Selin, Sigrid, 2024: Hur kan paleoekologiska studier hjälpa oss att bättre förstå hur de ekosystem vi anser skyddsvärda har formats och hur de bör vårdas? (15 hp)
682. Rey, August, 2024: Isrörelser och havstransgressioner speglade i Kåsebergåsen. (15 hp)
683. von Vultée, Anton, 2024: Babets kvarlevor - En morfologisk och sedimentologisk undersökning av överspolningssediment vid Tobisvik, Simrishamn. (15 hp)
684. Olsson Roso, Céline, 2024: Fåglarnas ursprung och tidiga utveckling. (15 hp)
685. Nawrocki, Bartosz, 2024: Karaktärisering av Cr-spinell i den ordoviciska Lokaformationen vid Skultorps stenbrott, Billingen. (15 hp)
686. Rydh, Alexander, 2024: Unraveling Magnetic Anomalies: A Study of Earth's Field Asymmetries during the Laschamps Excursion. (15 hp)
687. Svensson, Ludvig, 2024: Echoes of impact: A petrographic analysis and classification of impact breccias from Hummeln, Sweden. (15 hp)

LUNDS UNIVERSITET

**Geologiska institutionen**
**Lunds universitet**
**Sölvegatan 12, 223 62 Lund**